Hydrostatic levelling sensors based on extrinsic fibre Fabry-Perot interferometer technology

A. Herty, H. Mainaud Durand, CERN, Geneva, Switzerland
F. Boudin, Laboratoire de Géologie, CNRS, Ecole Normale Supérieure de Paris, France
H. C. Seat, M. Cattoen, F. Lizion, LAAS-CNRS, Université de Toulouse, INP, Toulouse, France
D. Boyer, A. Cavaillou, Laboratoire Souterrain à Bas Bruit, INSU-CNRS, Rustrel, France

Abstract

With the high luminosity upgrade of the Large Hadron Collider, the alignment monitoring systems in the Long Straight Sections around ATLAS and CMS will expect annual radiation doses of 100 kGy. Hydrostatic levelling systems will be deployed for vertical and tilt monitoring. To resist to these high radiation doses, the electronics have to be placed up to 200 m apart from the sensors. A candidate for this task is a hydrostatic levelling sensor based on extrinsic fibre Fabry-Perot interferometer technology. Any variation in the level of the reference surface is detected as a variation in the optical path length between the fibre probe situated in the sensor head and the mirror that is submerged in the liquid. In laboratory conditions the prototype was successfully operated in a range of 10 mm with a resolution of 5 nm. Thermal and atmospheric influences as well as the internal drift of the interferometer are compensated by the differential measurement carried out with a single laser source. The sensing fibre can be several kilometres long and the system allows signal processing up to 10 kHz. These design parameters have been tested in two field tests, one at the Laboratoire Souterrain à Bas Bruit for a sensor validation test. The other one at CERN in comparison with the currently used capacitive hydrostatic levelling sensor type. The results show that the technology can be applied for future hydrostatic levelling sensors. The approach to an absolute measurement solution is still under investigation.

PROJECT

The High Luminosity Large Hadron Collider (HL-LHC) is a project aiming to increase the total number of collisions by a factor of 10 beyond the nominal design value [1]. More accurate measurements of new particles and sensitivity increase are the main advantages of a more powerful LHC [2, 3]. In addition, the total luminosity of about 300 fb^{-1} received by the inner triplet quadrupoles by 2023 corresponds to a total radiation dose of 30 MGy. In order to anticipate a possible radiation damage failure of some components in the inner triplets, the magnets will be changed during the HL-LHC upgrade [4]. The alignment of final focus components in the Long Straight Sections around the experiments has to keep up with the new requirements. The zone of about 50 m around the experiments, that is currently equipped with permanent monitoring sensors, will be extended. More components with critical alignment tolerances will be installed in this high radiation area that will extend to 200 m on each side of the experiments. In the future, the monitoring system will cover the zone from Q1 to Q5 magnet.

The monitoring and alignment concept remains unchanged with respect to the concept presented by Coosemans et al. [5] and thus the same tolerances as specified in the LHC design report are kept [6]. The requirements for the hydrostatic levelling sensor to be used for the HL-LHC project are given in Table 1. Particular attention is drawn to the annual radiation dose, the interchangeability and the remote data acquisition requirements.

Table 1: sensor specifications

requirements	**quantification**
Annual / total radiation dose	100 kGy / 1 MGy
Magnetic field	insensitive
Range	$\geq$ 5 mm
Resolution	$\leq$ 0.2 µm
Interchangeability	$\leq$ 5 µm
Repeatability	$\leq$ 1 µm
Data acquisition frequency	$\geq$ 1 Hz
Drift	$\leq$ 1 µm per month
Inclination tolerance	$\leq$ 1 °
Remote data acquisition	$\geq$ 200 m from sensor
Compatibility to dimensions of current installation	
Type of sensing	contactless

Though the project seems to still be far away with an installation planned in 8 years' time; the need for development of a prototype is imminent for the concept validation. A full string test of the components of the interaction region is planned in 2021 implying that new sensors have to be available in pre-series stage by then. The installation of the HL-LHC components will take place from 2024 to 2026 and hence pave the way for an operation of the accelerator up to 2040 [2].

SENSOR DESIGN

At the heart of the HLS prototype is an extrinsic fibre Fabry-Perot interferometric (EFFPI) sensor which detects the variation in liquid levels in the sensing cavity to nanometric precision by measuring the optical path difference induced [7]. The EFFPI sensor is coupled to communicating hydrostatic vessels to form the optical interferometrically-interrogated HLS (iHLS), as schematically illustrated in Figure 1.

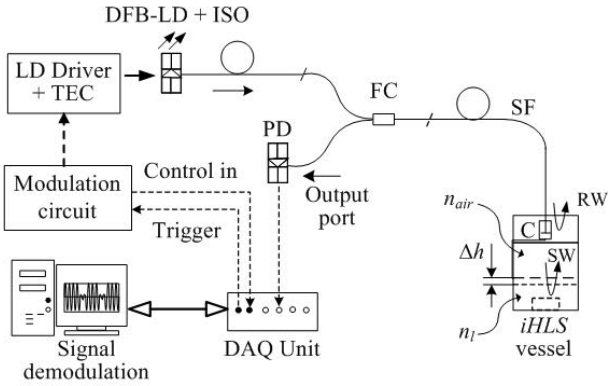

Figure 1: Schematic of iHLS incorporating an EFFPI sensor (ISO: integrated optical isolator, TEC: temperature regulator, DAQ: data acquisition).

The interrogating principle of the iHLS is based on the interference of two light waves at the end of the sensing fibre (SF). Monochromatic light from a temperature-regulated DFB-type laser diode is transmitted via a fibre circulator (FC) into the sensing fibre where a small percentage of the lightwave is reflected at the fibre end in the collimator (C) as the reference wave (RW) while the rest is transmitted as the sensing wave (SW) into the back-reflected sensing cavity to incident on a reflective surface. The sensing wave re-enters the sensing fibre and combines with the reference wave to produce interference. Any movement or displacement of the reflective surface, or equivalently, any variation in the optical cavity length such as induced by a variation in the liquid level will result in dynamic interference fringes being generated. This interference signal is then guided through the fibre circuit to the output port to be detected by a photodetector. In addition, a modulation scheme is applied to the laser drive current to obtain a pair of quadrature interference signals and for quasi-static measurements. The quadrature signals, can be written in the form of

$$V_x = V_{0x} + V_{mx} \cdot cos(\Delta\Theta) \quad (1)$$

$$V_y = V_{0y} + V_{my} \cdot sin(\Delta\Theta) \quad (2)$$

where, respectively, V_x and V_y are the detected quadrature pair, V_{0x} and V_{0y} their DC components and V_{mx} and V_{my} their fringe contrasts. The phase term $\Delta\Theta = \frac{4\pi}{\lambda} \cdot (n_l - n_{air}) \cdot \delta h$, with λ the interrogating wavelength, δh the level variation, n_l and n_{air} the refractive indices of the liquid and air medium, respectively, can then be demodulated using the incremental phase-tracking technique to extract the desired information, i.e. liquid level variation, through

$$h_i = h_{(i-1)} + \Delta\Theta_i \cdot \frac{\lambda}{4\pi(n_l - n_{air})} \quad (3)$$

with h_i the level at the i^{th} position and h_{i-1} that at the precedent position. The total variation measured is then simply the sum of h_i or $\Delta h = \sum_{i=0}^{n} h_i$.

TEST INSTALLATIONS

A validation campaign has first been carried out in the LAAS-OSE[1] laboratory to test and calibrate the complete iHLS instrument with preliminary investigation on the sensor linearity, inclination tolerance limits as well as the dynamic range of the iHLS.

Secondly, the system has been installed at LSBB[2] for comparison to a long base tiltmeter with a length of 148 m operating on hydrostatic measurements. This tiltmeter, the HLS-LINES system, is based on the same measurement principle as the iHLS, but uses a floating device in the liquid to amplify the height variation observed [8, 9]. The LSBB is a low background noise underground research site based on an old French military area covered by several hundreds of meters of solid rock. The chosen gallery is 250 m long and separated from the rest of the tunnel by several doors. The ambient temperature varies without interventions in the range of some hundredths of degrees Celsius per year. The installation of the iHLS used different fibre lengths between 130 m to 270 m as the electronics are installed outside the gallery.

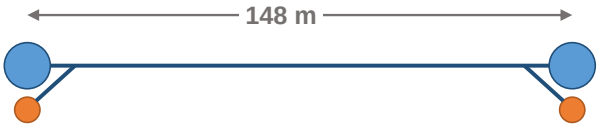

Figure 2: Layout of the LSBB set-up with HLS-LINES sensors (blue) and iHLS (orange).

As a final step, the system has been deployed in a test installation at CERN, allowing the comparison to the currently used capacitive hydrostatic HLS sensors (cHLS) and in a system configuration that simulates the main layout features of the LHC hydrostatic levelling network. In addition to a stability test, the sensors have been checked for linearity.

The test installation is a 110 m long hydrostatic network, shown in Figure 3, with three measurement stations. Each station can host a cHLS and an iHLS

[1]Laboratoire d'Analyse et d'Architecture des Systèmes - Optoélectronique pour les Systèmes Embarqués

[2]Laboratoire Souterrain à Bas Bruit

sensor. In order to vary the height of the liquid in the system, a filling-purging access is available. The system is designed as a half-filled system with a horizontal main pipe and individual connecting tubes that are connected separately for water and air to the measurement pots.

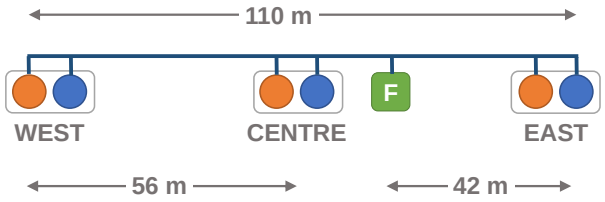

Figure 3: HLS test network in TT1 with the stations west, centre, east and the filling-purging access (F).

The sensing fibre has the same length for all stations of 250 m. Hence the 110 m installation simulates technically a longer network.

The test installation is in the TT1 tunnel, situated approximately 20 m underground. The temperature is stable to ±1°C during the year. The system has been operational with cHLS eight months before the start of the comparison measurements with the iHLS.

The cHLS sensor data is typically stored during stability measurements as the average of 30 measurements at 0.5 Hz data acquisition rate. For dynamic measurements the system is set to 0.2 Hz. The noise of the averaged signal is in the order of 1 µm. The iHLS data acquisition runs typically at 1 kHz and the measurements are downscaled to an averaged 4 Hz for analysis purposes.

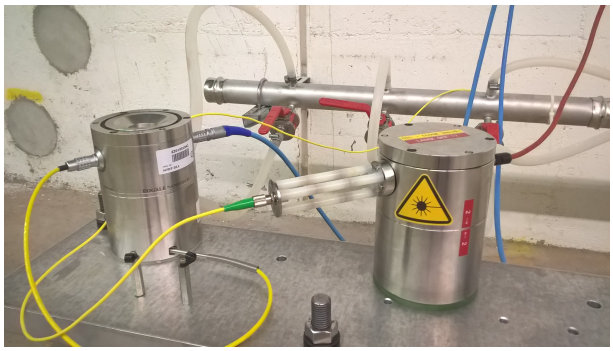

Figure 4: cHLS and iHLS installed on the common reference support in TT1 with the main hydraulic network in the background.

TEST RESULTS

Laboratory

Range and linearity. In the laboratory the range of the sensors was validated by injecting and extracting a precisely known volume of liquid. Two iHLS have been connected with flexible, full-filled tubes to a measurement pot used for varying the volume of the liquid. The left side of Figure 5 shows the complete cycle of injection and extraction with the small steps representing volumes of 5 ml and the larger steps volumes of 20 ml. The test results show that the sensor covers a measurement range of 10 mm. On the right hand side of the figure, a zoom on an injection of 5 ml is shown. This represents a height change of 249 µm and repeats for consecutive volumes to better than ±1 µm. This value obtained from the tests correcponds within 2 µm to the theoretically calculated value.

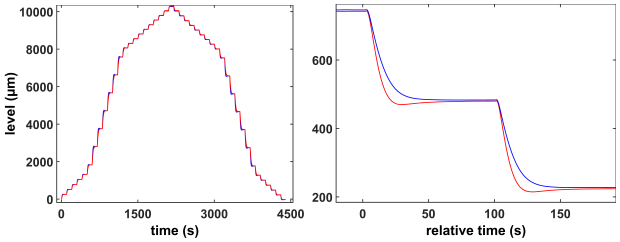

Figure 5: (left) iHLS range measurement by injection and extraction of liquid with two sensors (red and blue). (right) zoom on the level variations produced by liquid extraction of 5 ml.

Inclination tolerance. The roll angle alignment of the magnets causes changes in the vertical orientation of the sensor supports. Thus the determination of the impact on iHLS measurements has been tested.

Two sets of measurements have been conducted to evaluate the influence: one at an inclination angle of 0.4° and one at 1.33°. These inclinations have been tested at four azimuths of 0°, 90°, 180° and 270°. The tested iHLS is connected to a network with two reference iHLS that will remain stable.

In order to control the linearity of the sensor in an inclined position, 5 times 1 ml of liquid have been injected before extracting the total amount in a single step. The variations observed between the inclined and the reference sensors are less than 1 µm for each measurement. During the test at 1.33° an increased noise level has been observed caused by a power loss in the return signal.

LSBB

Stability and earth tides analysis. The stability measurements from the LSBB site showed that both sensors follow a variation of 20 µm within the $1\frac{1}{2}$ months observation period. The example given in Figure 7 shows differences between the sensors reaching up to 5 µm. This disagreement can be caused by the different methods of how the sensors are fixed to the rock.

The stability of the two systems can also be expressed by looking at the tilt calculated from the two sensors at the extremities.

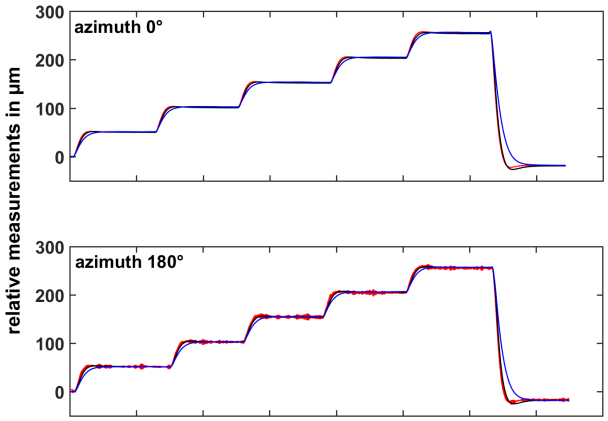

Figure 6: Test of inclination tolerance at 1.33° by successive injection and extraction of liquid to the system at two azimuth positions.

The differences in the earth tides observed by the system are described as a change of the tilt in Figure 8: +20 nrad per month for iHLS and -20 nrad per month for HLS-LINES. According to the length of the instrument, this tilt can be translated to a change of ± 3 µm for the sensors.

To control the amplitude of the earth tides, a spectrum analysis has been calculated with ETERNA 3.4 software [10]. The amplitude factor is used to evaluate each tidal wave amplitude observed with respect to the theoretical amplitude. For the M2 wave, the most significant semi-diurnal tidal, the ETERNA analysis calculated factors of 0.986 with 0.010 root mean square (RMS) for the HLS-LINES and 0.916 with 0.005 RMS for the iHLS.

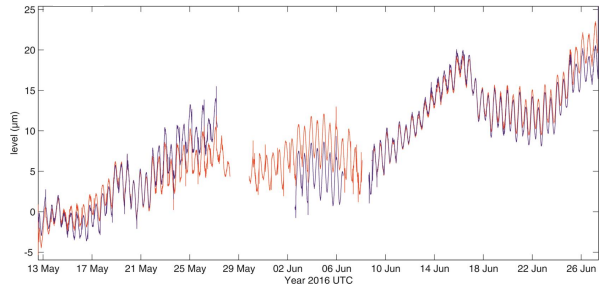

Figure 7: Comparison between the level variation of liquid recorded respectively by an iHLS (red) and an HLS LINES (blue).

CERN

System response and sensitivity. After the installation of cHLS and iHLS sensors at CERN, a system validation test was carried out. The aim of the test was to confirm the system response between the measurement stations, the determination of the damping behaviour of waves and the sensitivity of the system.

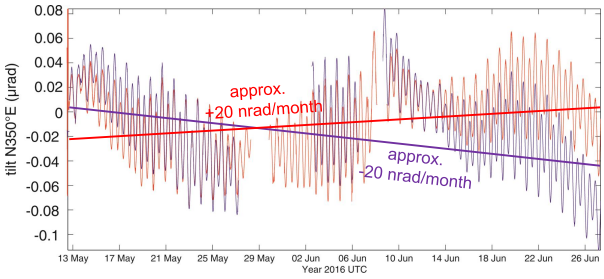

Figure 8: Comparison between the tilt of the long base tiltmeter HLS-LINES (blue) and the tilt from the iHLS (red).

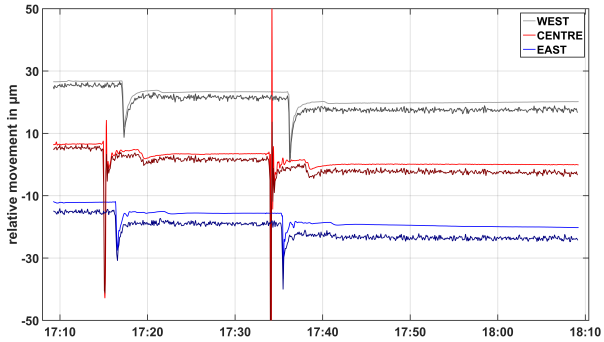

Figure 9: TT1 system response after injecting water at the filling-purging access of the network.

The graph presented in Figure 9 shows two injections to the system each with 20 ml of liquid. The height difference observed by the sensors is 3 µm. The wave front propagates from the filling-purging access to the sensor situated in the centre before reaching the east and west sensor. The relation of the observed wave travel time corresponds to the distance between the sensors. The system only shows one major wave before damping it down to the order of 0.5 µm at approximately 3 min after the first wave passed. The total stabilization time of the system is around 20 min.

Stability comparison. These initial stability measurements were carried out for a duration of $5\frac{1}{2}$ weeks after admitting a settling time of two weeks for the sensors after installation. The relative measurements of the three stations are shown in Figure 10.

The sensors situated at the west and east position see similar relative movements. The upwards displacement of 30 µm in the east position is seen by both sensors and is in agreement with observations from the nine months of stability measurements of the cHLS at this position. The sinusoidal signal of the sensors at the extremities corresponds to the earth tides.

The central sensor suffered from a stability problem which was voluntarily not fixed during the measurement campaign. The sensor's collimator has been

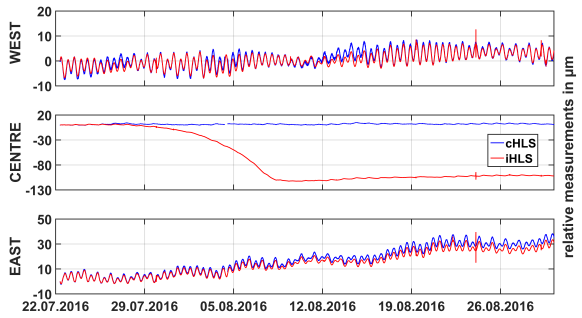

Figure 10: Stability comparison - relative measurements in TT1 with cHLS and iHLS.

cleaned during maintenance and the sensor now provides stable measurements. The source of the problem is resolved but not understood yet.

As amplitude and behaviour are considered to be similar, no significant difference in the stability of cHLS and iHLS can be observed.

Linearity validation. As described in the paragraph Range and linearity, a linearity calibration for the iHLS has been carried out in the laboratory. This calibration is compared to the cHLS sensors installed at CERN. Both types of sensors installed in this experiment have a range of 10 mm as shown in Figure 5 for the iHLS and as given by the manufacturer for the cHLS.

A partial linearity validation in the range of approximately 1.5 mm was realised in order to compare the linearity. This has been done by extraction and injection of liquid to the main hydraulic network. The results from Figure 11 show a difference between cHLS and iHLS as the curves do not superpose. For this test, only the west and east sensors are examined according to the results from the stability comparison. The zigzag steps during extraction and injection show partial volumes of 2 l that have been added or removed.

The observed differences are summarized in numerical form in Table 2. The height differences observed by the cHLS as well as by the iHLS are compared to each

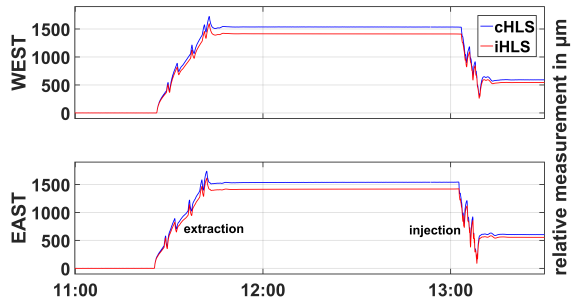

Figure 11: TT1 linearity validation.

other for each type of sensor. The difference between the height differences, $d_{E,W}$, is less than 5 µm and corresponds to less than 1 % of the variation observed, consequently the hydraulic network is communicating well.

The difference between the systems is presented in the colums $\Delta h(cHLS - iHLS)$ with Δh calculated as

$$\Delta h = cHLS - iHLS \tag{4}$$

according to each position in the network and relative to the type of variation carried out. An averaged scale factor of 7.92 % ± 0.08 % between cHLS and iHLS has been calculated.

The cHLS sensors have been tested independently for their linearity according to the check procedures implemented at CERN [11]. The linearity has been confirmed to be better than 2 µm along the range of 10 mm and thus the observed scale factor can be assigned to the iHLS.

The iHLS currently uses a protective oil layer on the water surface to minimize evaporation. The internal geometry of an iHLS vessel is for compatibility reasons similar to a cHLS vessel. The reflective surface of the iHLS is located in the oil layer. Taking into account the hydrostatic balance between an initial and a final state after injecting an amount of water, the hydrostatic pressure motion can be expressed as illustrated in Figure 12 by the initial (eq. 5) and the final state (eq. 6).

$$\rho_o \cdot g \cdot \Delta H_{o,1,i} + \rho_w \cdot g \cdot \Delta H_{w,1,i} = \rho_w \cdot g \cdot \Delta H_{w,2,i} \tag{5}$$

$$\rho_o \cdot g \cdot \Delta H_{o,1,f} + \rho_w \cdot g \cdot \Delta H_{w,1,f} = \rho_w \cdot g \cdot \Delta H_{w,2,f} \tag{6}$$

with the indices for the oil, o, and water layer, w, i describing the initial and f the final state. The relations between the initial state and the final state are expressed by the following equations:

$$\Delta H_{w,2,f} = \Delta H_{w,2,i} + \delta H_{w,2} \tag{7}$$

$$\Delta H_{w,1,f} = \Delta H_{w,1,i} + \delta H_{w,1} \tag{8}$$

$$\Delta H_{o,1,f} = \Delta H_{o,1,i} + \delta H_{o,1} \tag{9}$$

$$\delta H_{o,1} \cdot D_v^2 = \delta H_{o,1} \cdot (D_v^2 - D_m^2) \tag{10}$$

Combining equations 5 - 10, the height difference $\delta H_{o,1}$ can also be expressed as

$$\delta H_{o,1} = \frac{\rho_w}{\frac{\rho_w \cdot D_v^2}{(D_v^2 - D_m^2)} + \rho_o} \cdot \delta H_{w,2} \tag{11}$$

The height difference $\delta H_{o,1}$ can be solved by equation 11 to 0.894 µm, assuming the parameters $\delta H_{w,2}$ =1µm, $\rho_w = 1000 \frac{kg}{m^3}$, $\rho_o = 965 \frac{kg}{m^3}$, $D_v = 80$ mm and $D_v = 26$mm. The theoretical difference is hence 10.6 %.

The difference between iHLS and cHLS can be explained by the above derivation and hence be compensated for to better than 3 %.

Table 2: Linearity validation by means of liquid injection and extraction.

	cHLS			iHLS			Δh(cHLS-iHLS)			
	W	**E**	$\mathbf{d}_{(E,W)}$	**W**	**E**	$\mathbf{d}_{(E,W)}$	**W**	**E**	$\mathbf{d}_{(E,W)}$	Δ(%)
INJECTION 1	-598.6	-595.8	2.8	-551.0	-548.6	2.4	47.6	47.2	-0.4	7.93
EXTRACTION 1	1535.5	1539.0	3.5	1411.9	1416.8	4.9	-123.6	-122.1	1.5	7.99
INJECTION 2	-942.2	-937.3	4.9	-867.6	-863.1	4.5	74.5	72.9	-1.6	7.85

all measurements are given in µm

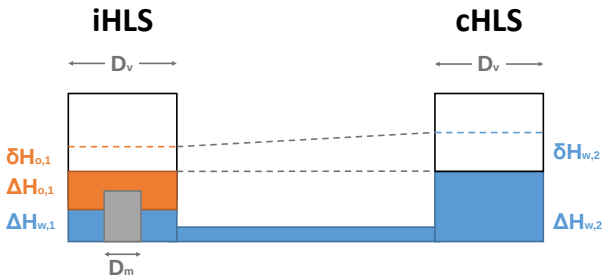

Figure 12: Parameters and schematics for hydrostatic pressure motion equations 5 - 11.

The phenomenon became noticeable in the CERN data following the large variation of the water level in the test. A closer analysis of the LSBB data revealed that a scale factor can also be identified in this data set. The residual discrepancy might be linked to the oil index that changes with respect to the manufacturer's specification as it is used in combination with water.

Seismic sensitivity. The HLS systems are based on a liquid level and hence subject to be influenced by vibrations. An earthquake is a typical example for such an effect allowing to put in evidence the influence on the measurement system and secondly the impact on a particle accelerator. During the stability tests two earthquakes have been registered. The passage of the waves is shown in Figure 13 as registered in the iHLS data. The distant earthquake happened on July 29, 2016 in the Mariana Islands region, situated at approximately 11500 km distance to CERN. The subduction zone earthquake with a magnitude of M7.8 generated surface waves that arrived several hours after the arrival of the initial seismic wave. The peak to peak perturbation observed in a measurement pot is in the order of 10 µm.

The lower part of Figure 13 is the August 24, 2016 earthquake that struck Central Italy with a magnitude of M6.2 at a distance of approximately 800 km from CERN. In this case the perturbation is around 30 µm peak to peak.

SUMMARY

The project has completed a full design and development chain within the last three years. The evaluation of the concept, the successful prototype building and testing in the laboratory was followed by two tests installations at LSBB and at CERN. The optical interferometrically-interrogated, contactless HLS confirmed its stability with respect to two other types of sensors.

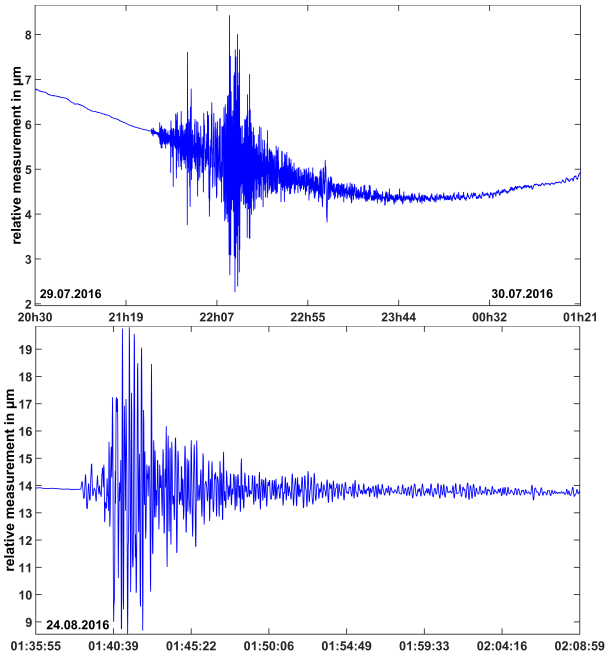

Figure 13: Earthquakes registered by iHLS: M7.8 earthquake in Mariana Islands region (top); M6.2 earthquake in Central Italy (bottom).

The linearity of the sensor has been calibrated in the laboratory with a known amount of liquid and checked with respect to a cHLS. A scale factor has been identified that can mainly be corrected for.

The development of the sensor has taken a major step by demonstrating that the sensor is capable of performing relative nanometre resolution measurements with a remote data acquisition of more than 250 m.

PERSPECTIVES

As the sensor fulfils most of the requirements - such as range, resolution, data acquisition frequency, remote data acquisition and inclination tolerance - the tests can now continue to investigate the long term stability of the sensor in the current installation. In

parallel, a particular focus has to be put in the near future on the radiation and magnetic field resistance of the sensor's components as well as towards an absolute measurement solution. The absolute measurement is of particular need for the future application in order to establish a permanent and stable reference between the EFFPI measurement and an external, geodetic reference on the sensor's housing.

Though the advantage of a remote data acquisition and the proof of principle given with the tests are a big step forward in the development of an iHLS sensor, the key feature necessary for future deployment at CERN will be the possibility to obtain absolute measurements with this sensor. This requirement is an essential constraint for a future use in the HL-LHC Long Straight Section monitoring project.

Further tests shall confirm if the suppression of the protective oil layer still allows reliable measurements of the sensor and hence should cancel the scale factor.

The system configuration with three prototype sensors has to be scaled to a LHC system configuration of up to 13 sensors in parallel with software implementations of automatic height difference calculation in accordance to the CERN technical network infrastructure.

REFERENCES

[1] G. Apollinari et al., "High-Luminosity Large Hadron Collider (HL-LHC): Preliminary Design Report". CERN, Geneva, Switzerland, 2015.

[2] L. Rossi and O. Brüning, "The High Luminosity Large Hadron Collider: the new machine for illuminating the mysteries of Universe". World Scientific, 2015, Advanced series on directions in high energy physics.

[3] L. Rossi, "LHC Upgrade Plans: Options and Strategy", Proceedings of IPAC2011, San Sebastian, Spain, 2011.

[4] I. Bejar Alonso and L. Rossi, "HiLumi LHC Technical Design Report". CERN-ACC-2015-0140, 2015.

[5] W. Coosemans et al., "The Alignment of the LHC Low Beta Triplets: Review of Instrumentation and Methods". 7th International Workshop on Accelerator Alignment, SPring-8, Japan, 2002.

[6] J.-P. Quesnel, "LHC Design Report - Volume II - Chapter 11". CERN, Geneva, Switzerland, 2004.

[7] H. C. Seat and M. Cattoen, "Dispositif à fibre optique extrinsèque pour la mesure d'un paramètre physique". Patent WO2012013698-2012-02-02, 2012.

[8] F. Boudin et al., "A silica long base tiltmeter with high stability and resolution". Review of Scientific Instruments, American Institute of Physics, 2008, 79, pp.4502.

[9] F. Boudin, "Development and validation of a mercury-silica long base tiltmeter for near surface measurement: application to geophysical measurements at high resolution at the experimental of the Gulf of Corinth". Ph.D. thesis, Université Paris, 2004.

[10] H.-G. Wenzel, "The nanogal software: Earth tide processing package ETERNA 3.30", Bulletin d'Information des Marées Terrestres (BIM), Bruxelles, No. 124, 9425-9439, 1996.

[11] A. Herty, A. Marin and H. Mainaud Durand, "Test and calibration facility for HLS and WPS sensors". 8th International Workshop on Accelerator Alignment, CERN, Switzerland, 2004.